# Ventricular fibrillation waveform properties influenced by thoracic impedance guided chest compressions in a porcine model

Computer Methods and Programs in Biomedicine 241 (2023) 107780

Contents lists available at ScienceDirect

Computer Methods and Programs in Biomedicine

journal homepage: www.elsevier.com/locate/cmpb

# Ventricular fibrillation waveform properties influenced by thoracic impedance guided chest compressions in a porcine model

Olibhéar McAlister [a,b,*], Adam Harvey [b], Ben McCartney [a,b], Paul Crawford [c], Raymond R Bond [a], Dewar D Finlay [a], David McEneaney [d]

[a] Ulster University, Belfast, UK
[b] HeartSine Technologies Ltd., Belfast, UK
[c] Veterinary Anaesthesia Consultancy, UK
[d] Craigavon Area Hospital, Craigavon, UK

ARTICLE INFO

*Keywords:*
Ventricular fibrillation
Thoracic impedance
Chest compressions
Quantitative waveform measures
Amplitude spectrum area
Mean slope

ABSTRACT

*Background and objective:* Quantitative measures extracted from ventricular fibrillation (VF) waveform reflect the metabolic state of the myocardium and are associated with survival outcome. The quality of delivered chest compressions during cardiopulmonary resuscitation are also linked with survival. The aim of this research is to explore the viability and effectiveness of a thoracic impedance (TI) based chest compression (CC) guidance system to control CC depth within individual subjects and influence VF waveform properties.

*Methods:* This porcine investigation includes an analysis of two protocols. CC were delivered in 2 min episodes at a constant rate of 110 CC $min^{-1}$. Subject-specific CC depth was controlled using a TI-thresholding system where CC were performed according to the amplitude ($Z_{RMS}$, 0.125 to 1.250 Ω) of a band-passed TI signal ($Z_{CC}$). Protocol A was a retrospective analysis of a 12-porcine study to characterise the response of two VF waveform metrics: amplitude spectrum area (AMSA) and mean slope (MS), to varying CC quality. Protocol B was a prospective 12-porcine study to determine if changes in VF waveform metrics, due to CC quality, were associated with defibrillation outcome.

*Results:* Protocol A: A directly proportional relationship was observed between $Z_{RMS}$ and CC depth applied within each subject ($r = 0.90$; $p < 0.001$). A positive relationship was observed between $Z_{RMS}$ and both AMSA ($p < 0.001$) and MS ($p < 0.001$), where greater TI thresholds were associated with greater waveform metrics. Protocol B: MS was associated with return of circulation following defibrillation (odds ratio = 2.657; $p = 0.043$).

*Conclusion:* TI-thresholding was an effective way to control CC depth within-subjects. Compressions applied according to higher TI thresholds evoked an increase in AMSA and MS. The response in MS due to deeper CC resulted in a greater incidence of ROSC compared to shallow chest compressions.

## 1. Introduction

Rapid defibrillation and the onset of early cardiopulmonary resuscitation (CPR) dramatically increases a patient's chance of surviving a cardiac arrest [1,2]. Current American Heart Association and European Resuscitation Council guidelines recommend chest compressions (CC) are provided at a rate of 100 to 120 CC $min^{-1}$ targeting a depth between 50 and 60 mm [3,4]. Rescuers have been reported to generally compress shallower than guideline recommendations; however, guideline rate adherence is high [5–7]. Finding the optimal CC depth for a given patient is an attractive prospect for resuscitation efforts particularly if this could be achieved using a measure of patient physiology.

The presence of ventricular fibrillation upon defibrillator deployment is associated with greater probability of survival [8]. VF waveform measures have been identified as predictors of defibrillation success and survival to hospital discharge. Common measures include amplitude spectrum area (AMSA) and mean slope (MS) [9–12], which represent the metabolic state of the myocardium [13].

Thoracic impedance (TI) is an electrophysiological signal primarily used in defibrillation for shock energy compensation [14]. During resuscitation, CC and ventilations cause artefacts in TI; therefore, filtering the signal can isolate this compression component ($Z_{CC}$). Alonso

* Corresponding author at: Ulster University, Belfast, UK.
*E-mail address:* olibhear.mcalister@stryker.com (O. McAlister).

https://doi.org/10.1016/j.cmpb.2023.107780
Received 23 March 2023; Received in revised form 17 August 2023; Accepted 24 August 2023
Available online 25 August 2023

et al. investigated the relationship between CC depth and TI waveform features in a clinical setting [15]. They discovered large variances in TI amplitude for a set CC depth applied across multiple patients. However, an analysis within the study found that given a wide spread of CC depths observed within a patient, the relationship between CC depth and TI amplitude may be directly proportional, therefore, a directional change in CC depth may result in a directional change in $Z_{CC}$ amplitude. This within-subject relationship between CC depth and TI has been observed in the pre-clinical setting when a range of CC depths were applied to a porcine model of cardiac arrest [16].

Understanding the dynamic nature of VF and its influencers during cardiac arrest and resuscitation may provide further insight to successful defibrillation and improved outcomes. The aim of the present investigation was to characterise the effect of CPR quality on the VF waveform measures and to determine if changes in AMSA and MS due to CC quality were reflected in defibrillation outcome. Within the scope of the present research the term CC quality refers to $Z_{CC}$ amplitude during manual CPR. The aim of this investigation was to evaluate changes in VF waveform properties when targeting specific $Z_{CC}$ amplitudes, causing a relative change in CC depth within individual subjects.

## 2. Material and methods

### 2.1. Study overview and ethics

The present research contains an analysis of two study protocols, one retrospective (A) and the other prospective (B), involving commercially sourced pigs subjected to cardiac arrest. Both studies were approved by The Roslin Institute, University of Edinburgh (Protocol A: Study number L330, 7th June 2018. Protocol B: Study number L369, 1st April 2019) and were monitored by independently by institute staff.

### 2.2. Study design

This investigation evaluated the VF waveform response to varying levels of CC quality. Endpoints AMSA and MS were derived from the VF waveform during a hands-off period, immediately after the cessation of CC. Each period of continuous CC was applied at a rate of 110 CC $min^{-1}$. Throughout the experiments CC quality was continually monitored using TI during CC. The studies in included in the present research were characterisation studies and therefore were not powered. Each study recruited 12 animals and utilised repeated measures design as appropriate, to reduce sample-size [17].

### 2.3. Chest compression guidance system

An application was developed to monitor fluctuations in TI during the application of CPR. Continuous measures of TI were captured using a multifunction I/O device (USB-6008; National Instruments, Austin, Texas) connected to a modified automated external defibrillator (AED; HeartSine Technologies Ltd., UK). A $Z_{CC}$ signal was derived from the TI signal by applying recursive second order Butterworth filters with high and low frequency cut-offs of 0.5 and 5 Hz, respectively. A 3-second buffer was applied to the $Z_{CC}$ signal where the root mean square (RMS) was extracted as a measure of amplitude ($Z_{RMS}$). $Z_{RMS}$ was displayed graphically on the user's screen using a series of light indicators, where the number of lights was proportional to the $Z_{RMS}$ value. An illustration of the chest compression guidance system is presented in Fig. 2 and the minimum $Z_{RMS}$ amplitude required to toggle each threshold level is listed in Table 1. This system was used to control the depth of CC within each animal. In addition, CC depth data was captured using an accelerometer-based Laerdal CPRmeter (Laerdal, Norway), connected to a Philips HeartStart MRx (Philips, Netherlands), and calculated post-experiment.

**Table 1**
Minimum impedance amplitude required to activate each threshold of the chest compression guidance system. The mean (standard deviation) of $Z_{RMS}$ and CC depth observed while targeting each threshold during protocol A are presented.

| Chest compression guidance system threshold | $Z_{RMS}$ threshold value, Ω | Mean $Z_{RMS}$ (SD), Ω | Mean depth (SD), mm |
|---|---|---|---|
| **1** | 0.125 | 0.18 (0.03) | 14.69 (4.13) |
| **2** | 0.250 | 0.35 (0.20) | 22.44 (4.38) |
| **3** | 0.375 | 0.41 (0.03) | 27.17 (5.06) |
| **4** | 0.500 | 0.55 (0.06) | 33.08 (5.66) |
| **5** | 0.750 | 0.82 (0.04) | 39.57 (5.15) |
| **6** | 1.000 | 1.00 (0.20) | 44.27 (6.39) |
| **7** | 1.250 | 1.25 (0.18) | 46.77 (5.89) |

### 2.4. Animal preparation

Once sedated, anesthetized, and intubated for mechanical ventilation and maintenance of anaesthesia, the study and veterinary team monitored physiological signs of the subjects. Prior to the induction of VF, electrodes connected to the AED were attached to the thorax of each animal in the sternum-apex position. The AED was responsible for recording high resolution ECG and $Z$ signals.

VF was electrically induced by placing a pacing wire in the right ventricle, via a jugular introducer sheath, and administering a 100 Hz current via a Grass Stimulator. Once VF was achieved, mechanical ventilation was stopped, and the animals were left to deteriorate in an untreated state of VF for 5 to 7 min. The untreated period of VF was used to represent VF waveforms after a prolonged response time during out-of-hospital cardiac arrest. Continuous CC were then applied to each of the animals after the elapsed period of untreated VF, at a target rate of 110 CC $min^{-1}$.

### 2.5. Protocol A

Twelve (12) pigs, with a mean (range) weight of 35.29 (33 to 37) kg, were enlisted for protocol A. Each animal was subjected to seven episodes of continuous CC, 2 min in duration, after an elapsed 7 min period of untreated VF. Quality of manual CC was randomized during the experiment by targeting a specific $Z_{RMS}$ amplitude range. Each $Z_{RMS}$ amplitude was targeted for a full 2 min episode of CPR. CC episodes were separated by a 10 to 15-second interval, indicative of an AED ECG analysis period. Calculations of AMSA and MS were made during these hands-off intervals. Once seven episodes of CC were applied to an animal the experiment was terminated and the animal was euthanized.

### 2.6. Protocol B

Twelve (12) commercial pigs were also enroled for protocol B, with a mean (range) weight of 30.75 (29 to 34) kg. Following 5 to 7 min of untreated VF, the animals were subject to a 2 min episode of manual CPR. There were three $Z_{RMS}$ thresholds targeted during the CPR episodes, 0.25 Ω, 0.50 Ω and 1.00 Ω. Defibrillation was attempted with a 150 J biphasic shock, following the cessation of CC.

Shock success was defined as termination of a shockable rhythm, for at least 5 s after shock delivery. Return of spontaneous circulation (ROSC) was defined as the restoration of a spontaneous (perfusing) rhythm, that results in more than an occasional gasp, fleeting palpated pulse, or arterial waveform.

When ROSC was achieved the animal was rested for 5 to 10 min and allowed to stabilise. An animal was deemed stable through monitoring of physiological signs. Once stable, VF was re-induced, and animals left in an untreated state for 5 to 7 min and the next CC threshold would be targeted.

If ROSC was not achieved, a rescue protocol was triggered to recover the animals according to the veterinary team's best practice. Escalating

shocks following a 150–150–200 J protocol were applied to the animals between rescue episodes. A rescue episode consisted of 2- min of CPR followed by a defibrillation shock, if appropriate. If ROSC was not achieved by the fourth rescue episode, the experiment was terminated, and the animal was euthanized. Timelines for both experimental protocols are presented in Fig. 1.

### 2.7. Post-event measurements

Electronic ECG and TI signals were downloaded from the AED after each event. Both signals were recorded with a sampling frequency of 250 Hz. A $Z_{CC}$ signal was derived from the downloaded TI data using the same method as the TI threshold system. $Z_{CC}$ data was annotated to locate the final compression present in each CPR episode and measures of $Z_{RMS}$ were calculated over a 15 s window immediately prior to the cessation of CC. Philips Event Review Pro-software was used to time-align the CC depth trace with the ECG and TI signals, by annotating the last compression in each CPR episode, and subsequently CC depth was calculated over the same 15 s period as $Z_{RMS}$.

Measurements of AMSA were calculated over a 512-sample (2.048 s) analysis window, starting at the point of annotation. Each AMSA value was obtained by taking the summation of the products of the observed amplitudes and frequencies between 4 and 48 Hz of a 1-sided fast Fourier transform (FFT). A Tukey window was applied to the ECG data prior to FFT application, to reduce edging effect.

$$AMSA\ (mV\ Hz) = \frac{2}{N}\sum_{i} A_i f_i,\ 4\ \text{Hz} \le f_i \le 48\ \text{Hz}$$

$N$ is the size of the FFT;
$A$ is a frequency bin amplitude (mV);
$f$ is a frequency bin frequency (Hz);
$i$ is a frequency bin index.

Mean slope was calculated over the same 512-sample window. This represents of the mean of the absolute first order derivative of the ECG signal.

$$MS\ \left(mV\ s^{-1}\right) = \frac{\sum_{i=\ 2}^{N} |ECG_i - ECG_{i-1}|}{N} fs$$

$ECG_i$ is an ECG sample amplitude (mV);
$N$ is the number of samples in the epoch;
$fs$ is the signal sample rate (Hz).

The time intervals for post-event feature extraction are presented in Fig. 3 and visualisations of AMSA and MS are shown in Fig. 4.

### 2.8. Statistical analysis

All analyses were conducted in Minitab (version 19.2; Minitab LLC, UK). Numeric baseline data were summarized by mean (standard deviation) or median (interquartile range). A Bland-Altman within-subject correlation [18] was applied to repeated measures of CC depth and $Z_{RMS}$ to establish the relationship between the numeric measures. Log transform was applied to the data to avoid non-normally distributed model residuals. AMSA and MS response to CC quality were analysed by applying a linear mixed effects model to the data. For data acquired under protocol A, subject identifier and duration of arrest were considered random-effects and $Z_{RMS}$, or CC depth were considered covariates.

For data acquired under protocol B, subject identifier and VF induction number were considered random-effects and TI threshold was considered a fixed effect. VF induction number was used as an indicator of prior resuscitation attempts, as it was assumed prior VF inductions and CPR would affect the ability to achieve shock success and ROSC. Coefficients for covariate endpoints are presented. Post-hoc Tukey pairwise comparisons test was applied to fixed effect factors. Counts of shock success and ROSC recorded under protocol B were tallied and presented as a fraction. A logistic regression model was subsequently applied to assess shock success and ROSC as a response of MS and AMSA. Odds ratios are presented for each model.

## 3. Theory

Intramyocardial adenosine triphosphate (ATP) levels have been shown to correlate with VF waveform properties [13]. The heart consumes ATP during VF to sustain electrical activity until its energy reserves have depleted [19]. By delivering CPR to a patient in cardiac arrest the rescuer is pumping oxygenated blood to the patient's ischaemic cardiac tissue, replenishing ATP available to the myocardium [20]. Depth of CC contributes to the volume of blood ejected from the heart with each compression [21]. We hypothesised that the depth of CC applied to a subject in VF would impact the rate of AMSA and MS decay. Therefore, the within-subject relationship between CC depth and $Z_{CC}$ may be used to control relative changes in CC depth and subsequently properties of the VF waveform.

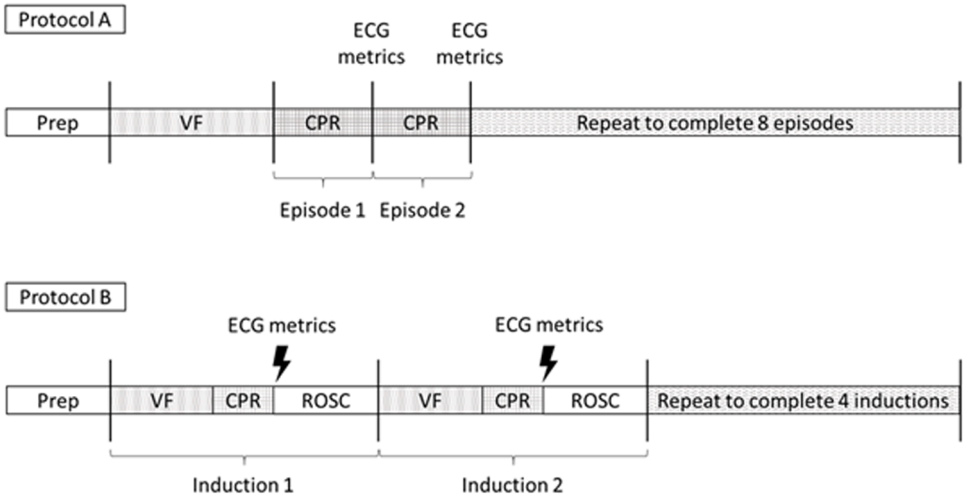


**Fig. 1.** Experimental timelines for protocols A and B. The duration of untreated VF was 5 to 7 min, and the duration of CPR was 2 min for both protocols. AMSA and MS were extracted from the ECG signal between CPR episodes in protocol A and immediately prior to shock delivery in protocol B. VF induction number is a sequential value where surviving animals were subjected to subsequent VF induction until ROSC could not be achieved.

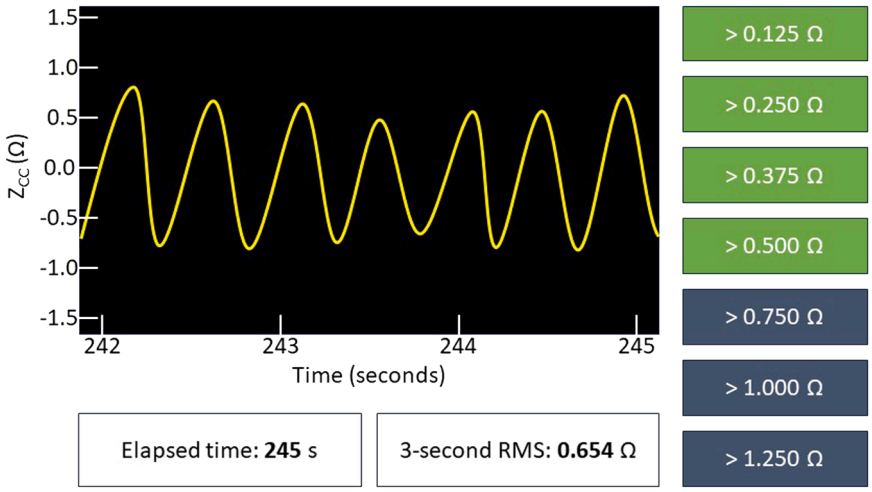


**Fig. 2.** Illustration of the thoracic impedance chest compression guidance system user interface. A main panel displays the $Z_{CC}$ signal in real-time. A 3-second RMS buffer is applied to the $Z_{CC}$ signal which illuminates a specific number of LEDs green on the right of the user interface.

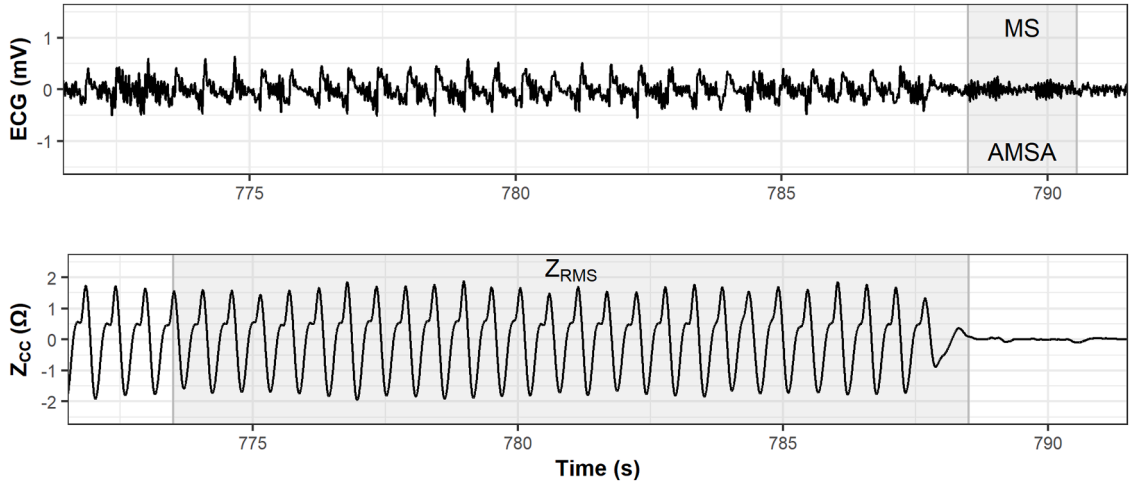


**Fig. 3.** Epoch of ECG and $Z_{CC}$ captured at the end of a 2 min episode of CPR. The highlighted regions demonstrate the time when signal features were extracted from the ECG (MS and AMSA) and $Z_{CC}$ ($Z_{RMS}$) signals relative to each other. The ECG analysis window occurs after the annotated point and the $Z_{CC}$ analysis occurs immediately prior to the annotation.

## 4. Results

### 4.1. Protocol A

The within-subject correlation (95% confidence interval; p-value) between the natural log of $Z_{RMS}$ amplitude and CC depth was 0.90 (0.85, 0.94; $p$ <0.001). Fig. 5 demonstrates the relationship between $Z_{RMS}$ amplitude and CC depth. No statistical difference was observed between CC depth achieved at each target $Z_{RMS}$ range between protocols ($p$ = 0.617).

Random intercept regression models were fitted to the AMSA and MS data as a response of time and either $Z_{RMS}$ or CC depth. Elapsed time from VF induction reduced AMSA by 0.36 mV Hz per min ($p$ <0.001) and MS by 0.24 mV $s^{-1}$ per min ($p$ <0.001). An increase in AMSA of 2.58 mV Hz ($p$ <0.001) and MS of 1.87 ($p$ <0.001) were observed per 1 Ω increase in targeted $Z_{RMS}$. Substituting $Z_{RMS}$ for CC depth within the regression models, corresponds to an increase in AMSA of 0.07 mV Hz and an increase in MS of 0.05 mV $s^{-1}$ for each 1 mm increase in CC depth. Subject identifier was determined to be a significant source of variance within the four regression models. Full details of the random-intercept models are presented in Table 2.

### 4.2. Protocol B

Compressions targeting $Z_{RMS}$ thresholds had an effect of AMSA ($R^2_{adjusted}$ = 0.480) and MS response ($R^2_{adjusted}$ = 0.465). A significant increase in AMSA (5.36 mV Hz; $p$ = 0.040) and MS (2.390 mV $s^{-1}$; $p$ = 0.038) were observed when targeting a $Z_{RMS}$ of 0.50 Ω compared to 0.25 Ω. No significant difference was observed in AMSA or MS between $Z_{RMS}$ targets of 0.50 Ω and 1.00 Ω or 0.25 Ω and 1.00 Ω. VF induction number and subject identifier did not have a significant effect on ASMA or MS response. A summary of CC and ECG endpoints are presented in Table 3.

Overall shock success was 77.42% (24/31) across all VF inductions and treatment levels throughout protocol B. Nine (9) of the 10 shocks delivered targeting 0.25 Ω, 7 of 9 shocks delivered targeting 0.50 Ω and 8 of 12 shocks delivered when targeting 1.00 Ω were successful. No association between $Z_{RMS}$ and shock success were observed (Fig. 6, $p$ = 0.424).

ROSC was observed after 25.81% (8/31) of the delivered shocks. Zero (0) of 10 shocks applied targeting 0.25 Ω, 5 of 9 shocks applied targeting 0.50 Ω and 3 of 12 shocks applied targeting 1.00 Ω resulted in ROSC. A significant difference in the incidence of ROSC between $Z_{RMS}$ was observed (Fig. 6, $p$ = 0.022).

There was no association between AMSA ($p$ = 0.613) or MS ($p$ =

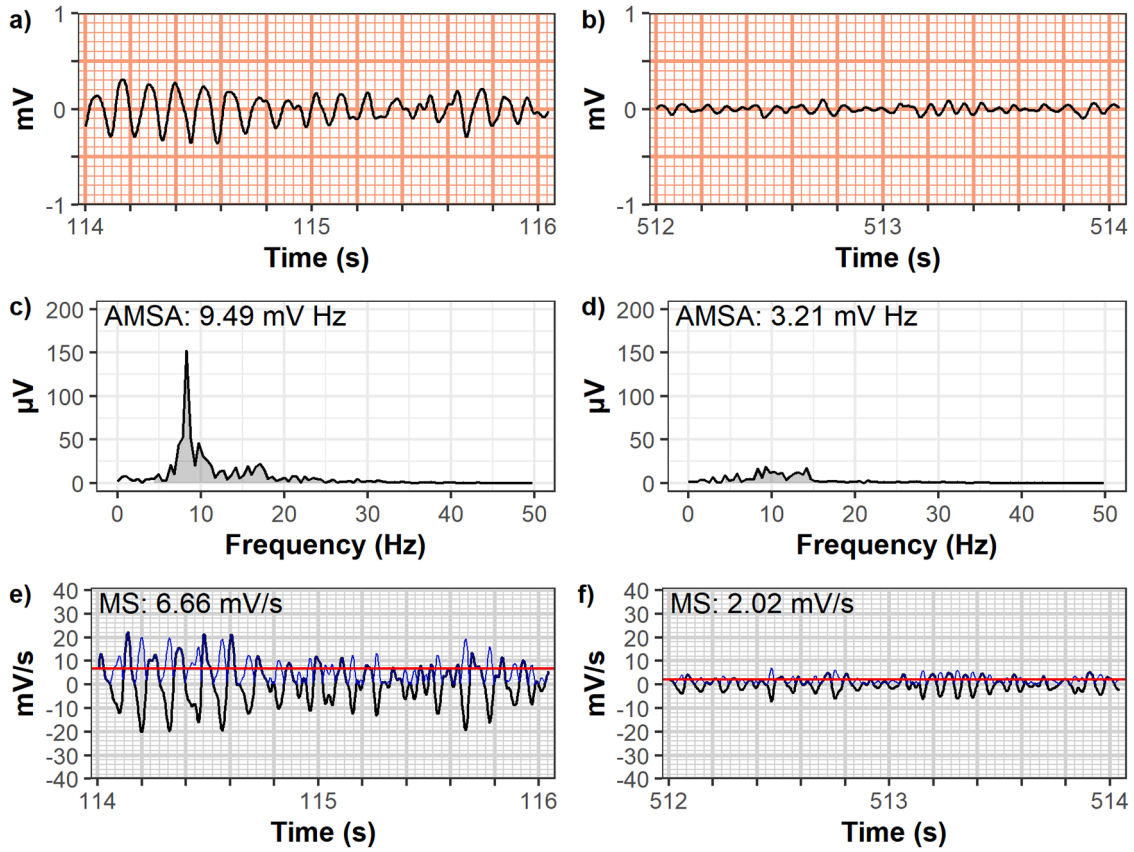


**Fig. 4.** Two ECG examples showing a) coarse and b) fine VF. Subplots c) and d) show the frequency spectrum, used to derive AMSA, which correspond directly to the ECG signals above. Subplots e) and f) display the first order time derivative of their respective VF signals, where absolute values of the derivative (blue) are used to calculate mean slope (red).

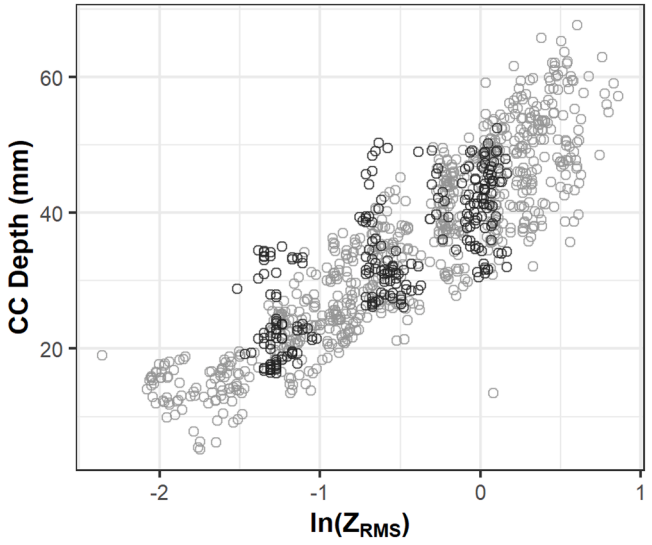


**Fig. 5.** Directly proportional relationship observed between $Z_{RMS}$ and CC depth using TI thresholding during protocol A (light grey) and protocol B (dark grey).

0.718) and shock success, after controlling for number of VF inductions. MS was identified as a significant predictor of ROSC ($p = 0.043$), with an odds ratio of 2.657 per 1 mV $s^{-1}$ rise. The odds ratio for AMSA as a predictor of ROSC was 1.701 per 1 mV Hz rise; however, this result was not statistically significant ($p = 0.054$).

**Table 2**
Protocol A: Random intercept ($u_i$) regression model summaries for AMSA and MS as a response of time, subject and either $Z_{RMS}$ or CC depth. The term $u_i$ represents between-subject variance, where $i$ is a subject specific index.

| Model variable | Coefficient | p-value |
|---|---|---|
| $AMSA_i = Time + Z_{RMS} + \mu_i$ | | |
| *Time ( min)* | −0.36 | <0.001 |
| $Z_{RMS}$ (Ω) | 2.58 | <0.001 |
| $u_i$ | – | <0.001 |
| $AMSA_i = Time + Depth + \mu_i$ | | |
| *Time ( min)* | −0.36 | <0.001 |
| *Depth (mm)* | 0.07 | <0.001 |
| $u_i$ | – | <0.001 |
| $MS_i = Time + Z_{RMS} + \mu_i$ | | |
| *Time ( min)* | −0.24 | <0.001 |
| $Z_{RMS}$ (Ω) | 1.87 | <0.001 |
| $u_i$ | – | <0.001 |
| $MS_i = Time + Depth + \mu_i$ | | |
| *Time ( min)* | −0.24 | <0.001 |
| *Depth (mm)* | 0.05 | <0.001 |
| $u_i$ | – | <0.001 |

## 5. Discussion

Within the present investigation, models were created for considering AMSA or MS as a response of time and TI amplitude changes due to applied CC depth. Both AMSA and MS decreased over time, due to VF being a time-sensitive arrhythmia shifting from coarse- to fine-VF eventually settling as asystole [22,23]. VF was analysed after at least 5- min of untreated VF and the reduction of AMSA and MS due to time was considered linear. This resulted in a decrease of 0.36 mV Hz or 0.24 mV $s^{-1}$ in AMSA and slope, for each elapsed min. However, the rate of

**Table 3**
Protocol B: summary of observations made during or immediately after the application of CC.

| Chest compression guidance system threshold | $Z_{RMS}$ threshold value, Ω | Mean $Z_{RMS}$ (SD), Ω | Mean depth (SD), mm | Mean AMSA (SD), mV Hz | Mean MS (SD), mV $s^{-1}$ |
|---|---|---|---|---|---|
| **2** | 0.250 | 0.29 (0.03) | 23.75 (6.31) | 12.58 (4.34) | 5.61 (2.07) |
| **4** | 0.500 | 0.53 (0.04) | 32.38 (6.07) | 18.12 (4.63) | 8.09 (2.18) |
| **6** | 1.000 | 0.91 (0.10) | 39.48 (5.75) | 15.67 (4.58) | 6.87 (1.96) |

reduction in AMSA and MS must be taken within the context of the present study as ECG acquisition methods, ECG epoch length and windowing functions applied to the data affect absolute values of VF waveform metrics.

The application of CPR had an effect on VF waveform measures where deeper CC increased both AMSA and MS [22,24]. A dose-response effect was found where $Z_{RMS}$ was directly related to the magnitude of VF waveform measures. The time-based decay in VF waveform measures was delayed or even reversed when greater TI thresholds were targeted. Relative changes in CC depth may be guided and monitored using the ECG and TI of a patient during CPR. This has application in the public access setting where bystander CPR can positively influence the survival outcome [25]. It has been previously reported that bystander CPR is suboptimal; however, programs such as despatch-assisted CPR have shown to improve bystander CPR engagement and confidence which boosts survival [25,26]. Guiding CPR using a patient's ECG and TI may prove a useful tool for bystander CPR engagement and provide feedback based on an electrophysiological response to CC.

Considering the relationship between the VF waveform measures and survival, efficacious CC depths early in a cardiac arrest event will produce an optimal VF response [27]. This early time period, however, is when VF is in an optimal state. Conversion to a perfusing rhythm, and thus survival, is most probable at this point so CC depth may not influence the outcome. For prolonged VF however, the prioritization of CPR may provide favourable outcomes. The metrics associated with survival are promoted during deep CC, therefore, if influencing VF score via CC quality does not confound their association with survival. This finding supports the concept that patients may benefit from a period of prolonged, deep, CC prior to defibrillation therapy presented by Aiello et al. [24], especially if the downtime of the patient is long or unknown.

There was a relationship between VF waveform measures and ROSC, but not for the termination of a shockable rhythm as previously reported [28]. No shocks which were delivered after the application of CC associated with the smallest $Z_{RMS}$ target resulted in a perfusing rhythm. The greatest proportion of shocks which resulted in ROSC was observed in the middle tier of $Z_{RMS}$ targets. A similar, yet non-significant, effect which may support observation is the recession in AMSA and MS response when targeting the greatest $Z_{RMS}$ threshold.

Although the incidence of ROSC was not significantly different between CC targeting 0.50 Ω and those targeting 1.00 Ω, the 0.50 Ω target did provide the greatest incidence of ROSC. A potential reason for the reduced rate of successful defibrillation for CC performed at 1.00 Ω may be due to excessive CC depth resulting in inter-thoracic damage [29,30]. Further research is required to explore this theory.

There was a significant increase in AMSA and MS when CC were applied targeting the 0.50 Ω tier compared to CC applied targeting 0.25 Ω. However, there was no measurable benefit to AMSA or MS when the $Z_{RMS}$ target was raised to 1.00 Ω. This may be indicative of a zone of "optimal" performance. CC applied at shallow depths – represented by the 0.25 Ω group – or excessive depths – represented by the 0.50 Ω group – may be of detriment to the quality of VF and subsequently the chance of achieving ROSC.

This investigation demonstrated that CC depth was effectively distributed by targeting a range of $Z_{RMS}$ thresholds. The relationship between depth and $Z_{RMS}$ was directly proportional within a given subject in line with previous findings [15,16]. Across the two reviewed investigations, TI proved an effective method for influencing CC depth to assess the effect of various CC depths on resuscitation outcomes. The relationship between TI and CC depth is expected to be affected by between-subject variability [16], therefore, the depth to achieve each of the $Z_{RMS}$ thresholds is an individualised indicator of CPR quality.

## 6. Conclusion

Amplitude and frequency characteristics of the VF waveform may be manipulated through the application of CC. Subject-specific CC depth was successfully controlled using the TI-based chest compression guidance system. There was a directly proportional relationship between CC depth guided by $Z_{RMS}$, and the VF waveform measures - AMSA and MS - extracted immediately after the cessation of CC. No association between applied CC depth and shock success was found; however, there was an association between CC depth and ROSC. The ECG may prove to be an indicator of resuscitation performance; therefore, a decision may be made via continuous monitoring of VF waveform measures during a resuscitation event.

## 7. Limitations

Within the present experiment the rate component to CC quality was not assessed, therefore, the effect of variable CC rate and chest recoil

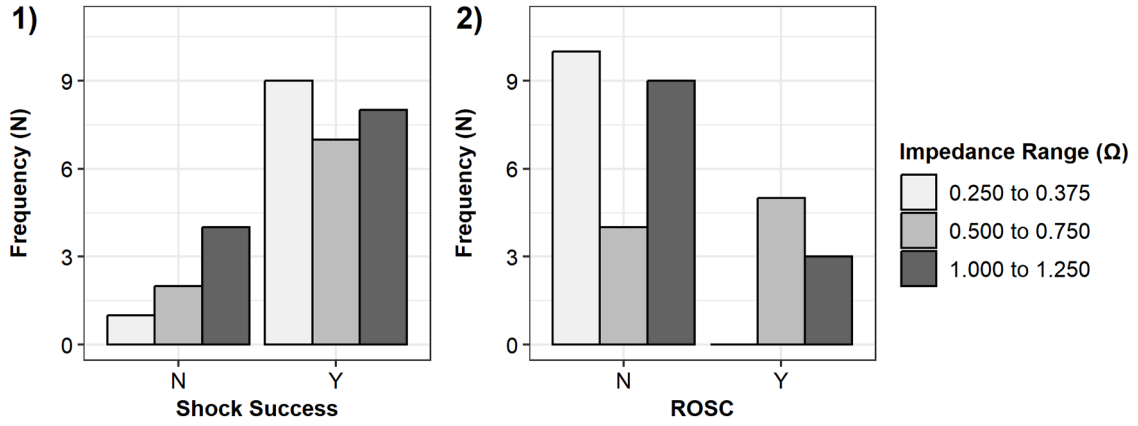


**Fig. 6.** The incidence of 1) of shock success and 2) return of spontaneous circulation (ROSC) following 150 J defibrillation shocks between each the three thoracic impedance ($Z_{RMS}$) thresholds during protocol B.

status on VF waveform metrics is unknown. Additionally, the effect of CC quality on VF was characterised after 5 to 7 min of untreated VF, thus, the results may not be applicable to shorter or longer durations of VF due to the changing rate of VF decay over time.

A relatively small sample was used in protocol B when observing binary endpoints of shock success, therefore, large effect sizes could be considered statistically significant. The experimental work conducted relates to an animal model of cardiac arrest, therefore, the effects highlighted are yet to be proven in a clinical setting.

## Declaration of Competing Interest

O. McAlister, A. Harvey and B. McCartney are employees of HeartSine Technologies Ltd. D. McEneaney is a medical advisor for HeartSine Technologies Ltd.

The presented research was fully funded by HeartSine Technologies Ltd. within the scope of an industrially sponsored PhD program.

## Acknowledgments

The authors of this paper would like to acknowledge the laboratory and veterinary staff at the Roslin Institute for their contribution and commitment to quality research. The present research was fully funded by HeartSine Technologies Ltd. within the scope of an industrially sponsored PhD program.

## References

[1] R.D. White, B.R. Asplin, T.F. Bugliosi, D.G. Hankins, High discharge survival rate after out-of-hospital ventricular fibrillation with rapid defibrillation by police and paramedics, Ann. Emerg. Med. 28 (5) (1996) 480–485, https://doi.org/10.1016/S0196-0644(96)70109-9. Nov.

[2] S.G.W. Lee, J.H. Park, Y.S. Ro, K.J. Hong, K.J. Song, S.D. Shin, Time to first defibrillation and survival outcomes of out-of-hospital cardiac arrest with refractory ventricular fibrillation, Am. J. Emerg. Med. 40 (2021) 96–102, https://doi.org/10.1016/j.ajem.2020.12.019. Feb.

[3] A.R. Panchal, et al., Part 3: adult basic and advanced life support: 2020 american heart association guidelines for cardiopulmonary resuscitation and emergency cardiovascular care, Circulation 142 (16_suppl_2) (2020) S366–S468, https://doi.org/10.1161/CIR.0000000000000916. Oct.

[4] T.M. Olasveengen, et al., European resuscitation council guidelines 2021: basic life support, Resuscitation 161 (2021) 98–114, https://doi.org/10.1016/j.resuscitation.2021.02.009. Apr.

[5] L. Wik, et al., Quality of cardiopulmonary resuscitation during out-of-hospital cardiac arrest, JAMA 293 (3) (2005) 299–304, https://doi.org/10.1001/jama.293.3.299. Jan.

[6] I.G. Stiell, et al., What is the role of chest compression depth during out-of-hospital cardiac arrest resuscitation?*, Crit. Care Med. 40 (4) (2012) 1192–1198, https://doi.org/10.1097/CCM.0b013e31823bc8bb. Apr.

[7] O. McAlister, et al., Temporal analysis of continuous chest compression rate and depth performed by firefighters during out of hospital cardiac arrest, Resuscitation (2023), 109738, https://doi.org/10.1016/j.resuscitation.2023.109738. Feb.

[8] J.P. Nolan, et al., Incidence and outcome of in-hospital cardiac arrest in the United Kingdom national cardiac arrest audit, Resuscitation 85 (8) (2014) 987–992, https://doi.org/10.1016/j.resuscitation.2014.04.002. Aug.

[9] H.P. Povoas, M.H. Weil, W. Tang, J. Bisera, K. Klouche, A. Barbatsis, Predicting the success of defibrillation by electrocardiographic analysis, Resuscitation 53 (1) (2002) 77–82, https://doi.org/10.1016/S0300-9572(01)00488-9. Apr.

[10] M. Shanmugasundaram, A. Valles, M.J. Kellum, G.A. Ewy, J.H. Indik, Analysis of amplitude spectral area and slope to predict defibrillation in out of hospital cardiac arrest due to ventricular fibrillation (VF) according to VF type: recurrent versus shock-resistant, Resuscitation 83 (10) (2012) 1242–1247, https://doi.org/10.1016/j.resuscitation.2012.02.008. Oct.

[11] G. Ristagno, et al., Amplitude spectrum area to guide defibrillation a validation on 1617 patients with ventricular fibrillation, Circulation 131 (5) (2015) 478–487, https://doi.org/10.1161/CIRCULATIONAHA.114.010989.

[12] A. Howe, et al., A support vector machine for predicting defibrillation outcomes from waveform metrics, Resuscitation 85 (3) (2014) 343–349, https://doi.org/10.1016/j.resuscitation.2013.11.021. Mar.

[13] D.D. Salcido, J.J. Menegazzi, B.P. Suffoletto, E.S. Logue, L.D. Sherman, Association of intramyocardial high energy phosphate concentrations with quantitative measures of the ventricular fibrillation electrocardiogram waveform, Resuscitation 80 (8) (2009) 946–950, https://doi.org/10.1016/j.resuscitation.2009.05.002. Aug.

[14] S.J. Walsh, et al., Efficacy of distinct energy delivery protocols comparing two biphasic defibrillators for cardiac arrest, Am. J. Cardiol. 94 (3) (2004) 378–380, https://doi.org/10.1016/j.amjcard.2004.04.042.

[15] E. Alonso, et al., Can thoracic impedance monitor the depth of chest compressions during out-of-hospital cardiopulmonary resuscitation? Resuscitation 85 (5) (2014) 637–643, https://doi.org/10.1016/j.resuscitation.2013.12.035.

[16] A. Howe, et al., An investigation of thrust, depth and the impedance cardiogram as measures of cardiopulmonary resuscitation efficacy in a porcine model of cardiac arrest, Resuscitation 96 (2015) 114–120, https://doi.org/10.1016/j.resuscitation.2015.07.020. Nov.

[17] S.A. Julious, Sample size of 12 per group rule of thumb for a pilot study, Pharm. Stat. 4 (4) (2005) 287–291, https://doi.org/10.1002/pst.185. Oct.

[18] J.M. Bland, D.G. Altman, Statistics notes: calculating correlation coefficients with repeated observations: part 1–correlation within subjects, BMJ 310 (6977) (1995), https://doi.org/10.1136/bmj.310.6977.446, 446–446Feb.

[19] K.B. Kern, et al., Depletion of myocardial adenosine triphosphate during prolonged untreated ventricular fibrillation: effect on defibrillation success, Resuscitation 20 (3) (1990) 221–229, https://doi.org/10.1016/0300-9572(90)90005-Y. Dec.

[20] T. Eftestøl, L. Wik, K. Sunde, P.A. Steen, Effects of cardiopulmonary resuscitation on predictors of ventricular fibrillation defibrillation success during out-of-hospital cardiac arrest, Circulation 110 (1) (2004) 10–15, https://doi.org/10.1161/01.CIR.0000133323.15565.75. Jul.

[21] C.F. Babbs, W.D. Voorhees, K.R. Fitzgerald, H.R. Holmes, L.A. Geddes, Relationship of blood pressure and flow during CPR to chest compression amplitude: evidence for an effective compression threshold, Ann. Emerg. Med. 12 (9) (1983) 527–532, https://doi.org/10.1016/S0196-0644(83)80290-X. Sep.

[22] Q. Yang, et al., Validation of spectral energy for the quantitative analysis of ventricular fibrillation waveform to guide defibrillation in a porcine model of cardiac arrest and resuscitation, J. Thorac. Dis. 11 (9) (2019) 3853–3863, https://doi.org/10.21037/jtd.2019.09.18. Sep.

[23] M.L. Weisfeldt, L.B. Becker, Resuscitation after cardiac arrest: a 3-phase time-sensitive model, JAMA 288 (23) (2002) 3035–3038, https://doi.org/10.1001/jama.288.23.3035. Dec.

[24] S. Aiello, et al., Real-time ventricular fibrillation amplitude-spectral area analysis to guide timing of shock delivery improves defibrillation efficacy during cardiopulmonary resuscitation in swine, J. Am. Heart Assoc. 6 (11) (2017) 14–20, https://doi.org/10.1161/JAHA.117.006749. Nov.

[25] Y.M. Park, S.D. Shin, Y.J. Lee, K.J. Song, Y.S. Ro, K.O. Ahn, Cardiopulmonary resuscitation by trained responders versus lay persons and outcomes of out-of-hospital cardiac arrest: a community observational study, Resuscitation 118 (2017) 55–62, https://doi.org/10.1016/j.resuscitation.2017.06.024. Sep.

[26] Y.S. Ro, et al., Effect of dispatcher-assisted cardiopulmonary resuscitation program and location of out-of-hospital cardiac arrest on survival and neurologic outcome, Ann. Emerg. Med. 69 (1) (2017), https://doi.org/10.1016/j.annemergmed.2016.07.028, 52-61.e1Jan.

[27] J. Thannhauser, et al., The ventricular fibrillation waveform in relation to shock success in early vs. late phases of out-of-hospital resuscitation, Resuscitation 139 (2019) 99–105, https://doi.org/10.1016/j.resuscitation.2019.04.010.

[28] D. Jin, et al., Does the choice of definition for defibrillation and CPR success impact the predictability of ventricular fibrillation waveform analysis? Resuscitation 111 (2017) 48–54, https://doi.org/10.1016/j.resuscitation.2016.11.022. Feb.

[29] D.D. Salcido, A.C. Koller, C. Genbrugge, E.L. Fink, R.A. Berg, J.J. Menegazzi, Injury characteristics and hemodynamics associated with guideline-compliant CPR in a pediatric porcine cardiac arrest model, Am. J. Emerg. Med. 51 (2022) 176–183, https://doi.org/10.1016/j.ajem.2021.10.030. Jan.

[30] H.Q. Zaidi, S. Li, D.G. Beiser, K.L. Tataris, W.W. Sharp, The utility of computed tomography to evaluate thoracic complications after cardiopulmonary resuscitation, Resusc. Plus 3 (2020), 100017, https://doi.org/10.1016/j.resplu.2020.100017. Sep.